Measuring dorsoventral pattern and morphogen signaling profiles in the growing neural tube

Marcin Zagorski[1] and Anna Kicheva[1]

[1]Institute of Science and Technology IST Austria, Am Campus 1, Klosterneuburg 3400, Austria

Correspondence: anna.kicheva@ist.ac.at

Running title: Measuring dorsoventral pattern in the neural tube

Attachments:

- Fiji script “maximum_projections.ijm”
- Fiji script “profile_quantification.ijm”
- Matlab script “data_analysis.m”
- Test dataset: folders “Images” and “Profiles_FI”

Measuring dorsoventral pattern and morphogen signaling profiles in the growing neural tube

Marcin Zagorski and Anna Kicheva

Abstract

Developmental processes are inherently dynamic and understanding them requires quantitative measurements of gene and protein expression levels in space and time. While live imaging is a powerful approach for obtaining such data, it is still a challenge to apply it over long periods of time to large tissues, such as the embryonic spinal cord in mouse and chick. Nevertheless, dynamics of gene expression and signaling activity patterns in this organ can be studied by collecting tissue sections at different developmental stages. In combination with immunohistochemistry, this allows measuring the levels of multiple developmental regulators in a quantitative manner with high spatiotemporal resolution. The mean protein expression levels over time, as well as embryo-to-embryo variability can be analyzed. A key aspect of the approach is the ability to compare protein levels across different samples. This requires a number of considerations in sample preparation, imaging and data analysis. Here we present a protocol for obtaining time course data of dorsoventral expression patterns from mouse and chick neural tube in the first three days of neural tube development. The described workflow starts from embryo dissection and ends with a processed dataset. Software scripts for data analysis are included. The protocol is adaptable and instructions that allow the user to modify different steps are provided. Thus, the procedure can be altered for analysis of time lapse images and applied to systems other than the neural tube.

Key Words

Neural tube, spinal cord, tissue development, morphogen gradient, pattern formation, quantitative imaging.

1. Introduction

Spinal cord development provides one of the best examples of developmental pattern formation. In this organ, an elaborate and stereotypic pattern of gene expression domains defines the identities of multiple neural progenitor subtypes along the dorsoventral (DV) axis [1]. This pattern is established in response to signaling by antiparallel morphogen gradients [2, 3] in a temporally dynamic manner. During the first three days of neural tube development in mouse and chick, the signaling gradients and the gene expression domains undergo considerable changes. At the same time, the tissue size increases from ~100μm to ~400μm. Although many signals and components of the gene network that defines neural tube patterning are known [1, 4–7], quantitative spatiotemporal measurements of their expression are to a large extent still lacking. The size of the tissue and developmental time scale make it difficult to study the temporal dynamics of patterning using live imaging. Hence, one of the best approaches remains the collection of transverse tissue sections through the spinal cord at different developmental time points. Such datasets allow quantifying the mean profiles and variation of signaling activity and gene expression along the DV axis over time [2, 3, 8, 9].

Here we describe how to prepare mouse and chick neural tube sections for immunohistochemistry, imaging and quantitative temporal analysis of dorsoventral signaling or gene expression profiles. The protocol builds on previous studies [2–4, 6] and is designed for stages between E8 and E11.5 of mouse embryonic development, or Hamburger-Hamilton (HH) stage 9 to HH stage 27 [10] in chick. We discuss key considerations in assigning developmental stage to tissue sections, sample processing, imaging and

data analysis that aim to minimize technical error and ensure that protein levels across different samples can be compared.

The first step is staging of the collected embryos and tissue sections. During development, the neural tube extends at the posterior end at the same time as new somites are added every 2h adjacent to it [11]. Both the neural epithelium and the adjacent somites continue to grow throughout development, but neuroepithelial and somite cells maintain approximate register along the anterior-posterior (AP) axis [12]. Thus, sections taken at the same somite number at different stage can be used to determine the behavior of the tissue over time. In practice, sections are collected from AP positions that encompass 3-4 somites, introducing size variability. However, the fact that anterior positions are developmentally older allows to correct for this variability by reassigning the developmental age of each measured profile based on the DV length of the tissue. The restaged sections can be later grouped into defined time intervals, so that temporal changes in the mean and variance of the expression profiles can be analyzed.

Once the embryos are collected, they are fixed, embedded in gelatin, cryosectioned and immunostained prior to imaging. To minimize the variability between samples that these steps could introduce, the samples are processed in parallel and the same batch of reagents are used for each time course experiment. In particular, all tissue sections are immunostained together and imaged in the same imaging session using identical settings. The images are then used to quantify the fluorescence intensity (FI) profiles within user specified regions of interest (ROI), which span the DV length of the neural tube. These profiles represent the average intensity across the ROI width for every pixel along the ROI length. Here we provide two Fiji macro scripts (see Methods 3.3) to facilitate measurement of the FI profiles.

The protocol presented here does not include a step in which immunofluorescence levels are directly calibrated to actual molecule numbers. Such calibration is possible for tagged proteins (see [13–15]) and can be easily incorporated into the protocol. Nevertheless, the protein levels can be compared in space

and time if the fluorescence intensity levels are proportional to protein levels. This requires linearity of antibody staining and fluorescence detection, which can be achieved with immunohistochemistry and laser scanning confocal microscopy [14–18]. Tests to ensure linear conditions [15, 17, 18] can be applied to the neural tube.

Further processing of the images in Matlab includes subtraction of background fluorescence, defined as the minimum intensity value in each profile, and removal of outlier profiles that deviate significantly from the mean profile for a given time window (see also [2, 19]). Outliers most often occur due to damage or distortions in the tissue sections that are caused by the dissection or sectioning procedure. Further corrections that can be optionally implemented include smoothing of the measured profiles and using a maximum projection of a small z-stack of images, rather than individual optical sections. These steps aim to correct for subcellular inhomogeneities of the signal that may arise from using stains that are restricted to the nuclei or cytoplasm. Thus, the signal is effectively averaged at a cellular scale to represent a continuum of DV positions across one cell diameter of the pseudostratified neural epithelium. Here we provide a Matlab script for processing of the measured profiles (see Methods 3.3).

The scripts and analysis steps are easy to modify and customize depending on the purpose of the analysis. The presented method can be directly used to study spatiotemporal changes in gene expression or activity of fluorescent reporters and biosensors. The approach can also be adapted to quantify fluorescence intensity profiles in the consecutive frames of time lapse recordings or to study correlations between fluctuations of two or more signals [3].

2. Materials

2.1. Equipment and software

1. Dissection scissors
2. Dumont #5 and #55 forceps, stainless
3. Disposable transfer pipettes, 7.5ml, 15.5cm
4. Two tungsten needles, each consisting of approximately 4cm of sharpened tungsten wire, 0.25mm diameter, mounted in a pin holder. To sharpen the wires, prepare a beaker with 5M KOH. From about 10cm of wire make several loops, attach to a negative electrode and immerse in the solution. Attach the 4cm piece of wire to be sharpened to the positive electrode. Set the voltage on a regulated DC power supply unit to a maximum of 4.5V and connect the electrodes. Dip the tip of the wire into the solution and hold until the desired sharpening or thinning of the wire is achieved (typically about a minute). Bend one of the needles ~0.5cm from the tip using forceps (to be used for dissection), and leave the other one straight (to be used for embedding).
5. Rocking platform
6. Disposable base molds (15x15x5 mm) for embedding
7. Low-temperature thermometer (-40°C)
8. Cryostat, Thermo Scientific Microm HM560 or equivalent
9. ImmunoPen™, Millipore
10. Plastic 5 microscope slide mailers (Leica) or equivalent
11. Laser scanning confocal microscope

12. Fiji software [20], http://fiji.sc/

13. Matlab software (MathWorks, MA, USA)

2.2. Reagents

1. Phosphate-buffered saline pH=7.4 (PBS), without Calcium and Magnesium salts

2. 4% paraformaldehyde in PBS

3. 15% sucrose in PBS

4. 7.5% gelatin from porcine skin, 15% sucrose in PBS. To prepare, warm up PBS to 70°C in a water bath. Slowly add gelatin from porcine skin (Sigma, G2500) to 7.5% and sucrose to 15% with occasional shaking. Leave on a hotplate with magnetic stirrer until sucrose and gelatin are completely dissolved. A well-mixed solution is essential for good results. Store 5ml aliquots at -20°C.

5. Isopentane

6. Washing buffer: PBS, 0.1% Triton-X-100

7. Blocking buffer: washing buffer, 1% (w/v) Bovine Serum Albumin

8. Primary antibodies

9. Fluorescent dye-conjugated secondary antibodies

10. 5mg/ml Dapi (4',6-diamidino-2-phenylindole), in dH_2O

11. ProLong Gold anti-fade mountant

3. Methods

3.1. Mouse/chick embryo preparation.

Perform all steps on ice using ice-cold reagents.

1. Dissect embryos in PBS, clearing all extraembryonic tissues (see **Note 1**).
2. Count and record the number of somites of each embryo. In wildtype litters, discard embryos that have not developed properly.
3. Remove the embryo heads. Using a plastic Pasteur pipette with a cut tip, transfer the embryos to a 2ml Eppendorf tube with PBS on ice (for stages corresponding to E10.5 (mouse) /HH17 (chick) or older, use a 5ml tube). If required, individual embryos can be processed separately (see **Note 2**).
4. Wash the collected embryos once with PBS.
5. Remove PBS and fill the tube with 4% paraformaldehyde. Fix on ice with slow rocking for the following amounts of time depending on the embryo stage: mouse E8.5 – 50min, E9.5 – 60min, E10.5 – 75 min, E11.5 – 90 min; chick HH8-11 – 50min; HH12-17 – 60 min; HH18-23 – 75min; HH23-27 – 90min.
6. Wash two times × 5 min with PBS.
7. Incubate at 4°C in PBS, 15% sucrose until embryos sink to the bottom of the tube (typically ~1h for E8.5, and up to overnight for older stages).
8. Defrost gelatin solution in a 42°C water bath and mix well. Fill a 2ml Eppendorf tube with 1ml of gelatin and keep on hot block at 38°C.
9. Using a tungsten needle with a bent tip, dissect the anterior-posterior region of interest, making a cut perpendicular to the dorsal midline. Perform the dissection in PBS, 15% sucrose (this step can also be performed in PBS prior to the sucrose incubation). Isolate pieces that are

approximately 7-10 somites long. For time course analysis, the same somite (e.g. somite #8 corresponding to brachial level in mouse) should be in the middle of the piece (Fig. 1A).

10. Using forceps, carefully transfer the embryo pieces into the gelatin. Wait a few minutes for them to sink to the bottom of the tube. Use separate tubes if embryos are processed separately (see **Note 2**).
11. Using a transfer pipette, transfer the embryos to an embedding mold and over-fill with gelatin. Orient the embryo pieces vertically with anterior facing down, ventral facing towards you (Fig. 1B). Arrange the pieces in an asymmetric pattern, so that each embryo can be clearly identified in different sections (Fig. 1, B and C, also see **Note 2, Note 3**). Keep orienting the pieces with a straight tungsten needle until the gelatin starts to solidify.
12. Once the gelatin has set, put the mold on ice and incubate for 30 min.
13. Remove the gelatin block from the mold and trim the block using a surgical blade. To mark the sample number and orientation, write a number directly on the gelatin block using a permanent marker or pen (test beforehand that the ink does not dissolve during freezing) (Fig. 1B).
14. Pour ~30ml of isopentane in a small beaker, place a thermometer in the solution and put on dry ice. As soon as the isopentane reaches -40°C, remove the thermometer and drop the gelatin block in the solution. Wait <1 min until the block is completely frozen, then use tweezers to transfer the frozen block to a tube and store at -80°C until ready to section. Do not allow the block to stay in isopentane for too long, or it will crack.
15. At the cryostat, mount the block so that sectioning starts from the anterior ventral side of the embryos and the DV axis is aligned orthogonal to the blade (see **Note 3**). Cut 12-14μm slices at -20°C and collect on 6-8 microscope slides. Alternate slides after every section, so that every anterior-posterior level is equally represented on every slide. Store slides at -80°C until ready to use.

3.2. Immunohistochemistry and imaging

Carry out the procedures at the specified temperature.

1. Sections from different stages that will be compared have to be stained together and imaged in the same imaging session in order to minimize technical error. Reserve a time slot on the confocal microscope of 4-8 h depending on the number of slides and experience of the user. Imaging should be performed between 2h and no more than 1 week from staining the slides.
2. Defrost and dry the slides with embryo sections for 10-15 min at room temperature.
3. Draw a hydrophobic boundary at the edge of each slide with ImmunoPen. To remove the gelatin from the sections, immerse the slides in slide containers filled with pre-warmed PBS in a 42°C water-bath and incubate for 20 min.
4. Wash once with warm PBS.
5. Wash with cold washing buffer.
6. Transfer the slides in a horizontal position to a chamber lined with wet paper towel for humidification. Immediately cover the slides with blocking buffer and incubate for 1h at room temperature in a closed chamber. It is critical that solutions are exchanged quickly and the sections are never left to dry during the entire procedure.
7. Prepare a master mix of primary antibody in blocking buffer for all slides. The optimal concentration of antibody should be determined before starting the time course experiment (see **Note 4**). Remove the blocking buffer and dispense 200μl or master mix per slide. Make sure the ImmunoPen border is intact. Incubate at 4°C overnight. Primary antibody may be reused several times.
8. Wash three times × 5 minutes in washing buffer.

9. Prepare a master mix of secondary antibody and Dapi in blocking buffer. Remove washing buffer and dispense 200µl or master mix per slide. Incubate 2h at room temperature.
10. Wash 3 times × 5 minutes in washing buffer.
11. Remove washing buffer. Dispense 2-3 drops (~15µl) of ProlongGold mounting medium at different positions in the slide. Using forceps, slowly lower a 24x60mm coverslip on the slide, avoiding bubbles. Store at 4°C until ready for imaging (up to 1 week after embedding).
12. At the confocal microscope, adjust the imaging field of interest in a way that fits the largest tissue (latest stage). This approach allows imaging the entire DV length of the neural tube of mouse embryos between E8.5 and E11 of development using a HCX Plan APO CS 40X Oil / 1.25 NA objective or equivalent.
13. Adjust the laser power and detection settings so that images from earliest, middle and latest developmental stages are not saturated and no signal above background is lost. Quantify the fluorescence intensity profiles recorded at different settings in order to determine the optimal settings (also see **Note 4**).
14. Once the imaging conditions are set, image the sections from all stages, focusing on the sections that were collected at the middle of the block in order to minimize variations in anterior-posterior positions (Fig. 1C). To record the fluorescence across ~1 cell diameter in AP direction, collect z-stacks of three optical slices, 1µm apart. For subsequent analysis using the provided scripts, the files should be named as "file_name_XXss.tif" (see **Note 5**) where XX is a two digit number indicating the somite stage (for stages 1 to 9, use 01 to 09).

3.3. Data processing

Two Fiji scripts, one Matlab script and a test dataset containing images and the corresponding raw FI profiles are provided for use in conjunction with the following steps.

1. In Fiji, open the "maximum_projections.ijm" script from the File menu and run it. An input folder containing the images saved as .tif files, and an output folder will be requested. The script will save the maximum projections of the files in the user specified directory without displaying the images.
2. In Fiji, open the "profile_quantification.ijm" script from the File menu. Open the maximum projections one by one in Fiji. For each image, run the Fiji script. You will first be prompted to draw an arrow from the floor plate to the roof plate, in order to rotate the image dorsal up, with the central lumen vertically aligned (Fig. 1D, 2A).
3. The second prompt asks the user to specify ROIs for quantification by adding them in the ROI manager. An example ROI of *width* = 12μm and *height* = 'DV length', positioned adjacent to the lumen, is shown in Fig. 2A. Two such ROIs per section can be used for quantifying gene expression patterns and morphogen activity profiles in the neural tube. However, the dimensions, position and number of ROIs can be chosen by the user depending on the experimental aims. After pressing OK, the FI profiles are recorded as .txt files in a user specified directory. The mean pixel intensity across the ROI in x-direction is quantified as function of *DVposition* in y-direction. The ventral midline corresponds to *DVposition*=0. *DVposition* is quantified in units of μm, using the scaling information embedded in the image. Before performing next step, check whether the resulting files contain data from all relevant images (see **Note 6**).
4. From this step onwards, the data analysis can be implemented by following the steps described below using any appropriate software. Alternatively, the Matlab script "data_analysis.m"

provided with this protocol can be used and modified as needed. The script contains an initial section where user-defined values of variables can be specified based on the descriptions provided in the remainder of the protocol. Run script "data_analysis.m". First, the user will be prompted to select the folder with .txt files containing the FI profile quantifications obtained with "profile_quantification.ijm" script. After pressing "Select Folder" all imported data should be in the 'profiles_raw' structure in the Matlab workspace (Fig. 2B).

5. The data is smoothed with a moving average filter (Fig. 2C). By default the smoothing window is set to 5µm, which corresponds roughly to one cell diameter. To modify the size of the smoothing window, change the value of the 'smooth_window' variable. The smoothing step can be omitted by commenting out the relevant part of the script (see **Note 7**).
6. The background fluorescence intensity is removed for each profile by subtracting the minimum intensity of that profile (see **Note 8**).
7. Specify somite stage for each imported file in the 'ss_time' array. The script can also automatically retrieve somite stage from the file names ('filenames' array) if the default naming convention is used (see Methods 3.2, step 14).
8. Restage the profiles by their DV length. To do this, first the exponential function $L(t) = L_0 \exp(t_{ss}/\tau)$ is fitted to the data, where L is the measured DV length, τ is a fit parameter and the time t_{ss} is determined as the somite stage × 2h/somite (Fig. 3A). The reassigned time $t(L)$ for each profile is determined via the inverse function, $t(L) = \tau \log(L/L_0)$, and is stored in the 'dv_time' array (see Fig. 3B, and **Note 9**).
9. To study temporal changes in gene expression, it may be practical to look at the average profiles in defined time intervals. To do this, specify time intervals over which the data should be averaged. The time intervals should be chosen manually (t_1, t_2, t_3, in Fig. 3B) in the 'time_intervals' array, or other strategies can be implemented (see **Note 10**). Once the profiles

are grouped into separate time intervals, the data is independently processed within each interval.

10. To analyze DV positions in units relative to the total DV length, DV positions are divided by the DV length of the profile. Profiles from different stages will have different resolution of positions. To compare profiles between stages, the resolution is unified by linear interpolation (see **Note 7** and **Note 10**).
11. The profiles (in units of relative DV position) are averaged for every time interval. The resulting mean profiles are in the array 'profile_mean0'.
12. The background of the mean profile for each time interval is subtracted (see **Note 11**).
13. The dorsal most and ventral most 5% of DV positions are excluded from subsequent analysis. In some cases these boundary regions can bias the subsequent processing steps (see Fig. 3C, **Note 12**).
14. Each profile is linearly rescaled to maximize its similarity to the mean profile, quantified by an R^2 coefficient (see **Note 13**). Profiles with R^2 below a user-defined threshold (variable 'R2_threshold' in the script) are discarded (see **Note 13)**. A new mean profile is calculated and the procedure iterated until no more profiles are discarded (Fig. 3D).
15. All profiles in the dataset are normalized by a common factor, so that the maximum mean profile intensity in the dataset is equal to 1 (Fig. 3E).

4. Notes

1. Embryo dissection. Mouse: Detailed description available in [21]. Briefly, remove the uterus and transfer to ice-cold PBS. Isolate the decidua by removing the muscle layer of the uterus using forceps. Starting from the mesometrial pole, dissect the deciduum to release the embryo.

Remove extraembryonic tissues. Chick: detailed description available in [22]. Briefly, remove 3-5ml of albumin using a syringe. Cut a window on the upper side of the egg using bent surgical scissors. Cut approximately 1cm around the embryo, holding the extraembryonic membranes on one side with forceps. Lift and transfer the embryo to a Petri dish with ice-cold PBS. Remove all extraembryonic tissues using micro-scissors and forceps.

2. Litters with mixed genotypes. After dissection, each embryo can be transferred to a separate well of a 48-well plate (for E11.5 – use a 24 well plate) filled with 0.5ml ice-cold PBS per well. The fixation, washing and sucrose steps are performed in the multi-well plate. Make sure the embryos are fully immersed in buffer at all times. For genotyping, collect the yolk sac for each embryo in an Eppendorf tube with a corresponding number. The yolk sacs can be stored at -20°C until ready for genotyping. For embedding, each embryo is dissected and transferred to a separate numbered 2ml Eppendorf tube with ~250µl gelatin. The embryos are then carefully transferred to the gelatin mold, keeping the order and arranged in a manner that allows unambiguously distinguishing the numbering.
3. Sectioning. Embedding and cryosectioning could introduce deformations of the tissue sections or deviations from orthogonality, i.e. the right angle between the section (DV axis) and the AP axis. To avoid these, a sharp blade without any notches or defects should be used. A blunt blade will tend to squash and fold the tissue sections. The alignment of embryos in the gelatin is also key - straight and precise dissection line helps to keep the embryo pieces upright. At the cryostat, the block should be aligned such that the first sections are cut from the center of the block. Sections cut at an angle that deviates from orthogonality may have DV lengths that are significantly larger and ratios of apicobasal width to DV length that differ from the average for a particular stage. This may lead to incorrect restaging of the sections by DV length **(Note 9).** Significant deviations are likely to become obvious upon inspection of the slide at the

microscope, as well as during the automatic discarding of outliers **(Note 13)**. However, small deviations can still remain undetected. For many gene expression patterns, analysis of the FI profile as a function of relative, rather than absolute, position along the DV axis alleviates this problem.

4. Optimizing immunostaining and imaging conditions. Primary antibody concentration and approximate imaging settings should be determined in a preliminary experiment. Slides containing adjacent sections from the same embryos are stained with a dilution series of antibody. The spatial resolution, scanning speed, averaging and bit-depth are selected (in our experience 1024 x 1024 pixels, pixel dwell time 1.58μs, 4 line averages and 8-bit image depth produce good results). The slides are then imaged with several settings of laser power and detector gain. The fluorescence intensity profiles are quantified, background subtracted (as described in Methods 3.3, steps 1-3, 6), normalized to the maximum FI of each profile and compared. The optimal conditions are the ones that give the lowest background fluorescence within the tissue without loss of signal. The signal is assessed by inspecting the detectable spatial differences in FI across the profile. Signal that is too low will result in loss of spatial differences in the low range of fluorescence intensities within the profile, whereas too high signal will result in saturation and loss of spatial differences in the high range of FI. Performing this analysis for developmental stages that contain the highest and lowest levels of signal ensures that the analysis spans the full dynamic range of intensity levels within the dataset. Whenever possible, linear relationship between protein levels and fluorescence intensity should be tested with a tagged version of the protein (see [16]). Furthermore, confocal detection in the linear range should be ensured using stepwise photobleaching or calibration assays [15].
5. File formats. Microscope-specific file formats can be opened in Fiji as hyperstacks using the Bio-formats plugin. Hyperstacks can then be saved as .tif files. We recommend automating this

conversion using a custom Fiji macro (examples can be found through the Fiji help menu, e.g. see http://imagej.nih.gov/ij/macros/BatchConvertToJPEG.txt).

6. FI profile files. The intensity profiles are recorded in *n* output files per active image, where *n* is the number of specified ROIs. In each file, the first column stores the DV position in units of pixels across the ROI in y-direction. The second column ("DVposition(μm)") stores distance in μm from the ventral midline (*DVposition*=0) across the ROI. The following columns store mean intensity values for the corresponding DV position in the respective channels. Each row corresponds to the mean intensity of pixels across the width of the ROI in x-direction. In addition to the .txt files, maximum projections of the z-stacks and ROIs are saved in corresponding subfolders.
7. Smoothing. Smoothing the FI profiles increases the robustness of subsequent steps of background subtraction and rescaling to relative DV positions. The profiles are rescaled to a predefined number of relative spatial positions (by default 100) by linear interpolation. If the original spatial resolution of the FI profiles is much denser than the resolution in relative units, many points will not be used in the rescaling. Smoothing counteracts this effect by locally averaging the FI values around rescaled positions. The default smoothing window of 5μm corresponds approximately to 1% DV length for late stages of neural tube development. The smoothing step could affect the magnitude of estimated variance, hence it can be modified or omitted (follow instructions within script to comment it out).
8. Background subtraction. By default the ventral- and dorsal-most 10% of DV positions are excluded for background determination. This improves the subtraction procedure for profiles where the intensity levels are high close to the two poles. This exclusion principle should be modified depending on the expected expression pattern, so that regions containing background fluorescence are not excluded. This can be done in the script by modifying the variables

'excludeV_bg=0.1' and 'excludeD_bg=0.9' accordingly as well as in the inequalities including these variables.

9. Restaging by DV length. The default initial values for the fit parameters are 'L_0=100' and 'tau_0=10'. Adjusting these parameters might be necessary for the fitting procedure to converge to the best fit. In the unlikely case that some profiles have smaller DV lengths than L_0 from the fit, the relation $t(L) = \tau \log (L/L_0)$ would result in negative developmental time (t<0) for these profiles. This is corrected by assigning t=0 to these profiles.
10. Time interval binning. For data points that are approximately uniformly distributed within the analyzed time period, binning can be done with fixed time intervals, e.g. every 10 hours. However, if some bins contain significantly fewer profiles than the others, this might affect the accuracy of the estimated mean and variance for these bins. In such cases, we recommend collecting more data focusing on the underrepresented intervals (see **Note 14**). Another strategy [18] is to define the time intervals so that every interval contains the same number of profiles. In this case, care should be taken that some time intervals do not become too large, obscuring relevant temporal changes.
11. Background of mean profiles. This step is optional, as background subtraction at the level of single profiles is often sufficient. However, averaging of profiles within time intervals reduces fluctuations, hence the background of the mean profile can be more precisely established. By default the same regions are excluded from the analysis as in the background subtraction step at the level of single profiles (see **Note 8**).
12. Excluding boundary regions. This step is optional and can be omitted. By default it keeps for analysis only the region between relative DV positions 'cutV=0.05' and 'cutD=0.95'. These values correspond approximately to the size of the floor plate and roof plate and can be modified as

needed. Note that the relative positions are not rescaled as a result of the exclusion, but the omitted points are simply not plotted.

13. Discarding outliers. This step is optional (follow instructions within the script to leave it out) and should be used when the analysis is targeted to mean profiles. It is used to discard outliers in a systematic way. Both R^2 maximization [2] and Y-alignment [3, 19, 23] can be used. These procedures are similar. In our experience, R^2 maximization results in a smaller percent of discarded profiles (<5% for threshold R^2=0.5) and fully conserves the mean profile at a given somite stage. By contrast, Y-alignment is more stringent, discarding 10-20% of the profiles for threshold R^2=0.5. Both procedures are insensitive to small spatial fluctuations, but are not suitable for small sample sizes, large variation between profiles, time intervals that are too large, and non-uniform distribution of the data. In R^2 maximization, the objective function $F(a_1, \dots, a_k) = \sum_{i=1}^{k}[1 - \frac{\sum_x (m_x - a_i\, p_x^i)^2}{\sum_x (m_x - \bar{m})^2}]$ is maximized for each time interval. Here a_i is an unknown scaling factor, *k* number of profiles in the time interval, p_x^i denotes the fluorescence intensity of the *i*th profile at relative DV position x, $m_x = \frac{1}{k}\sum_{i=1}^{k} p_x^i$ is the mean intensity at x in that time interval, and $\bar{m} = \frac{1}{DVR}\sum_x m_x$ is mean of intensities at all positions and all profiles in this time interval, excluding the boundary regions (see **Note 12**). The objective function can be interpreted as a sum of R^2 for separate profiles linearly rescaled to best reproduce the mean profile for the corresponding time interval. In practice, the fit parameters $(a_1, \dots, a_k)$ are first estimated with the least-square method to best reproduce the mean profile. Next, profiles with R^2 below a predefined threshold are discarded one by one. The mean profile without rescaling is recalculated after every step and discarding is repeated until all R^2 are above threshold. The fraction and quality of the discarded profiles should be inspected to determine a threshold R^2 value. The number of samples per time interval should be such that the mean profile does not change significantly if individual profiles are removed after the discarding procedure.

14. Pooling datasets. To increase the sample sizes, it is sometimes necessary to collect time course data in several experiments. The sample preparation and imaging conditions should still be the same for all experiments. To pool together the data from different experiments, first determine the 90th percentile of the fluorescence intensity of each profile χ, which represents a robust estimate of the maximum signal. The separate time-course datasets are then normalized relative to the median χ in each dataset. This normalization typically reduces the difference between the means of two experiments to levels much below the variation coefficients of the individual datasets.

Acknowledgements

We thank J. Briscoe and T. Bollenbach for comments on the manuscript. Funding: IST Austria and European Research Council under European Union's Horizon 2020 research and innovation programme (680037) (MZ, AK).

References

1. Alaynick WA, Jessell TM, Pfaff SL (2011) SnapShot: Spinal cord development. Cell 146:178 . doi: 10.1016/j.cell.2011.06.038

2. Kicheva A, Bollenbach T, Ribeiro A, Valle HP, Lovell-Badge R, Episkopou V, Briscoe J (2014) Coordination of progenitor specification and growth in mouse and chick spinal cord. Science 329:1466–1468 . doi: 10.1126/science.

3. Zagorski M, Tabata Y, Brandenberg N, Lutolf MP, Tkačik G, Bollenbach T, Briscoe J, Kicheva A (2017) Decoding of position in the developing neural tube from antiparallel morphogen gradients. Science 356:1379–1383 . doi: 10.1126/science.aam5887

4. Briscoe J, Pierani A, Jessell TM, Ericson J (2000) A homeodomain protein code specifies progenitor cell identity and neuronal fate in the ventral neural tube. Cell 101:435–445 . doi: 10.1016/S0092-8674(00)80853-3

5. Oosterveen T, Kurdija S, Alekseenko Z, Uhde CW, Bergsland M, Sandberg M, Andersson E, Dias JM, Muhr J, Ericson J (2012) Mechanistic Differences in the Transcriptional Interpretation of Local and Long-Range Shh Morphogen Signaling. Dev Cell 23:1006–1019 . doi: 10.1016/j.devcel.2012.09.015

6. Balaskas N, Ribeiro A, Panovska J, Dessaud E, Sasai N, Page KM, Briscoe J, Ribes V (2012) Gene Regulatory Logic for Reading the Sonic Hedgehog Signaling Gradient in the Vertebrate Neural Tube. Cell 148:273–284 . doi: 10.1016/j.cell.2011.10.047

7. Peterson KA, Nishi Y, Ma W, Vedenko A, Shokri L, Zhang X, McFarlane M, Baizabal JM, Junker JP, van Oudenaarden A, Mikkelsen T, Bernstein BE, Bailey TL, Bulyk ML, Wong WH, McMahon AP (2012) Neural-specific Sox2 input and differential Gli-binding affinity provide context and positional information in Shh-directed neural patterning. Genes Dev 26:2802–2816 . doi: 10.1101/gad.207142.112

8. Junker JP, Peterson KA, Nishi Y, Mao J, McMahon AP, van Oudenaarden A (2014) A predictive model of bifunctional transcription factor signaling during embryonic tissue patterning. Dev Cell 31:448–460 . doi: 10.1016/j.devcel.2014.10.017

9. Cohen M, Kicheva A, Ribeiro A, Blassberg R, Page KM, Barnes CP, Briscoe J (2015) Ptch1 and Gli regulate Shh signalling dynamics via multiple mechanisms. Nat Commun 6:1–12 . doi: 10.1038/ncomms7709

10. Hamburger V, Hamilton H (1951) A series of normal stages in the development of the chick embryo. J Morphol 88:49–92

11. Gomez C, Özbudak EM, Wunderlich J, Baumann D, Lewis J, Pourquié O (2008) Control of segment number in vertebrate embryos. Nature 454:335–339 . doi: 10.1038/nature07020

12. Stern CD, Jaques KF, Lim TM, Fraser SE, Keynes RJ (1991) Segmental lineage restrictions in the chick embryo spinal cord depend on the adjacent somites. Development 113:239–244

13. Lippincott-Schwartz J, Presley JF, Zaal KJ, Hirschberg K, Miller CD, Ellenberg J (1998) Monitoring the dynamics and mobility of membrane proteins tagged with green fluorescent protein. Methods Cell Biol 58:261–281 . doi: 10.1016/S0091-679X(08)61960-3

14. Kicheva A, Pantazis P, Bollenbach T, Kalaidzidis Y, Bittig T, Jülicher F, González-Gaitán M (2007) Kinetics of Morphogen Gradient Formation. Science 315:521–525 . doi: 10.1126/science.1135774

15. Kicheva A, Holtzer L, Wartlick O, Schmidt T, González-Gaitán M (2013) Quantitative imaging of morphogen gradients in

drosophila imaginal discs. Cold Spring Harb Protoc 8:387–403 . doi: 10.1101/pdb.top074237

16. Gregor T, Wieschaus EF, McGregor AP, Bialek W, Tank DW (2007) Stability and Nuclear Dynamics of the Bicoid Morphogen Gradient. Cell 130:141–152 . doi: 10.1016/j.cell.2007.05.026

17. Morrison AH, Scheeler M, Dubuis J, Gregor T (2012) Quantifying the Bicoid morphogen gradient in living fly embryos. Cold Spring Harb Protoc 7:398–406 . doi: 10.1101/pdb.top068536

18. Dubuis JO, Samanta R, Gregor T (2013) Accurate measurements of dynamics and reproducibility in small genetic networks. Mol Syst Biol 9:639 . doi: 10.1038/msb.2012.72

19. Gregor T, Tank DW, Wieschaus EF, Bialek W (2007) Probing the Limits to Positional Information. Cell 130:153–164 . doi: 10.1016/j.cell.2007.05.025

20. Schindelin J, Arganda-Carreras I, Frise E, Kaynig V, Longair M, Pietzsch T, Preibisch S, Rueden C, Saalfeld S, Schmid B, Tinevez J-Y, White DJ, Hartenstein V, Eliceiri K, Tomancak P, Cardona A (2012) Fiji: an open-source platform for biological-image analysis. Nat Methods 9:676–682 . doi: 10.1038/nmeth.2019

21. Behringer R, Gertsenstein M, Nagy K (2013) Manipulating the Mouse Embryo: A Laboratory Manual, Fourth. Cold Spring Harbor Laboratory Press New York

22. Bronner-Fraser M (2011) Avian embryology, 2nd edition. Methods Cell Biol 87:1–409

23. Tkačik G, Dubuis JO, Petkova MD, Gregor T (2015) Positional information, positional error, and readout precision in morphogenesis: a mathematical framework. Genetics 199:39–59 . doi: 10.1534/genetics.114.171850

Figure legends

Fig. 1. Sample preparation. **A)** The brachial region of the embryo is dissected out by cutting along the red lines. **B)** The dissected pieces are embedded in the indicated orientation in an asymmetric pattern. The number '1' (or any asymmetric symbol) is written on the block to mark the orientation after freezing. **C)** The block is sectioned in A to P direction and the sections collected on 6-8 microscope slides. Sections corresponding to somite positions in the center of the dissected region are located in corresponding positions on the slides (red arrows). Each embryo can

be unambiguously identified across sections. **D)** Close-up of a transverse section of the neural tube, showing the pseudostratified epithelium. The red rectangle is the ROI used for measuring the fluorescence intensity.

Fig. 2. Fluorescent intensity profile quantification. **A)** Maximum projection image of the neural tube, dorsal side up, stained for Dapi (channel 1), pSmad (channel 2), GFP (GBS-GFP [6], channel 3), Nkx2.2 and Pax3 (channel 4). The ROI outlined in yellow is 12 µm wide and spans the DV length of the neural tube as indicated. Scale bar, 10 µm. **B)** FI profiles quantified from the images in A as the mean FI across the ROI width for each *DVposition* along the ROI length (y direction). *DVposition* = 0 corresponds to the ventral boundary of the ROI. **C)** The FI profiles from B are smoothed with moving average filter of 5 µm and background subtracted.

Fig. 3. Mean profile time course for a test dataset. **A)** DV length as a function of $t_{ss,}$ time derived from somite stage. Fitting $L(t) = L_0 \exp(t_{ss}/\tau)$ to the data (circles) yields parameter values $L_0 = 54.8 \pm 3.8$ µm and $\tau = 29.0 \pm 1.1$ h. **B)** Restaged profiles (see Note 9). The profiles were binned into consecutive time intervals denoted by t_1, t_2, t_3. **C)** Mean profile (black) for all profiles (red, gray) in the t_1 time interval. The profiles were rescaled to relative *DVposition*, the background of the mean profile was subtracted, and the dorsal- and ventral-most 5% of DV positions were excluded. **D)** R^2 maximization with $R^2 < 0.5$ resulted in discarding the dashed gray profile in C in the first iteration. All profiles had $R^2 > 0.5$ in the second iteration. **E)** Mean profiles for all time intervals for all analyzed channels. The mean profiles were normalized to the maximal mean intensity in the time course dataset.

Figure 1

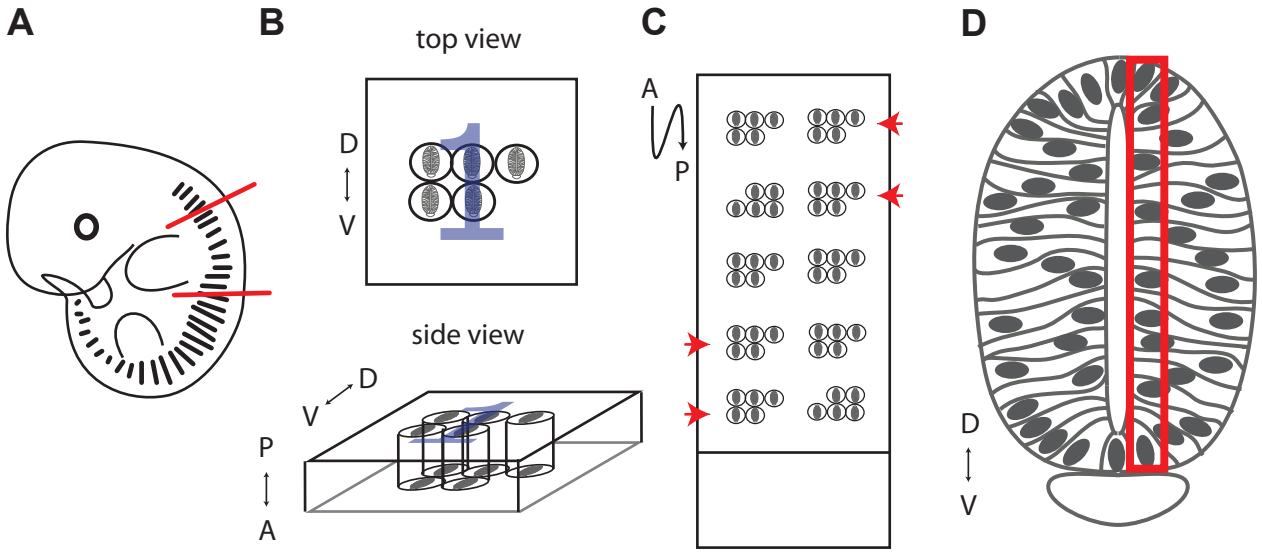

Figure 2

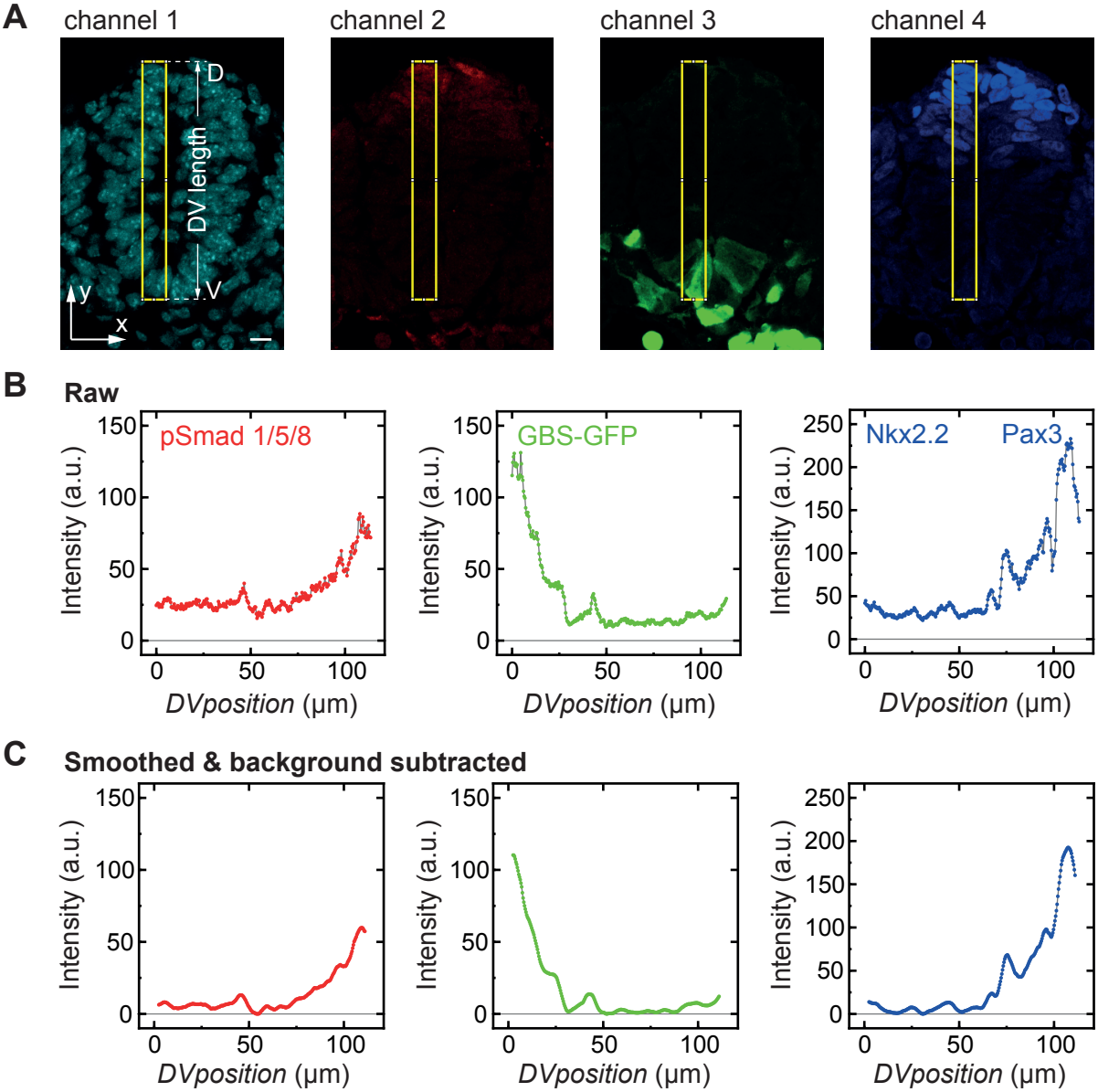
A
channel 1
channel 2
channel 3
channel 4
D
DV length
V
y
x
B
Raw
pSmad 1/5/8
GBS-GFP
Nkx2.2
Pax3
Intensity (a.u.)
DVposition (μm)
C
Smoothed & background subtracted
Intensity (a.u.)
DVposition (μm)

Figure 3

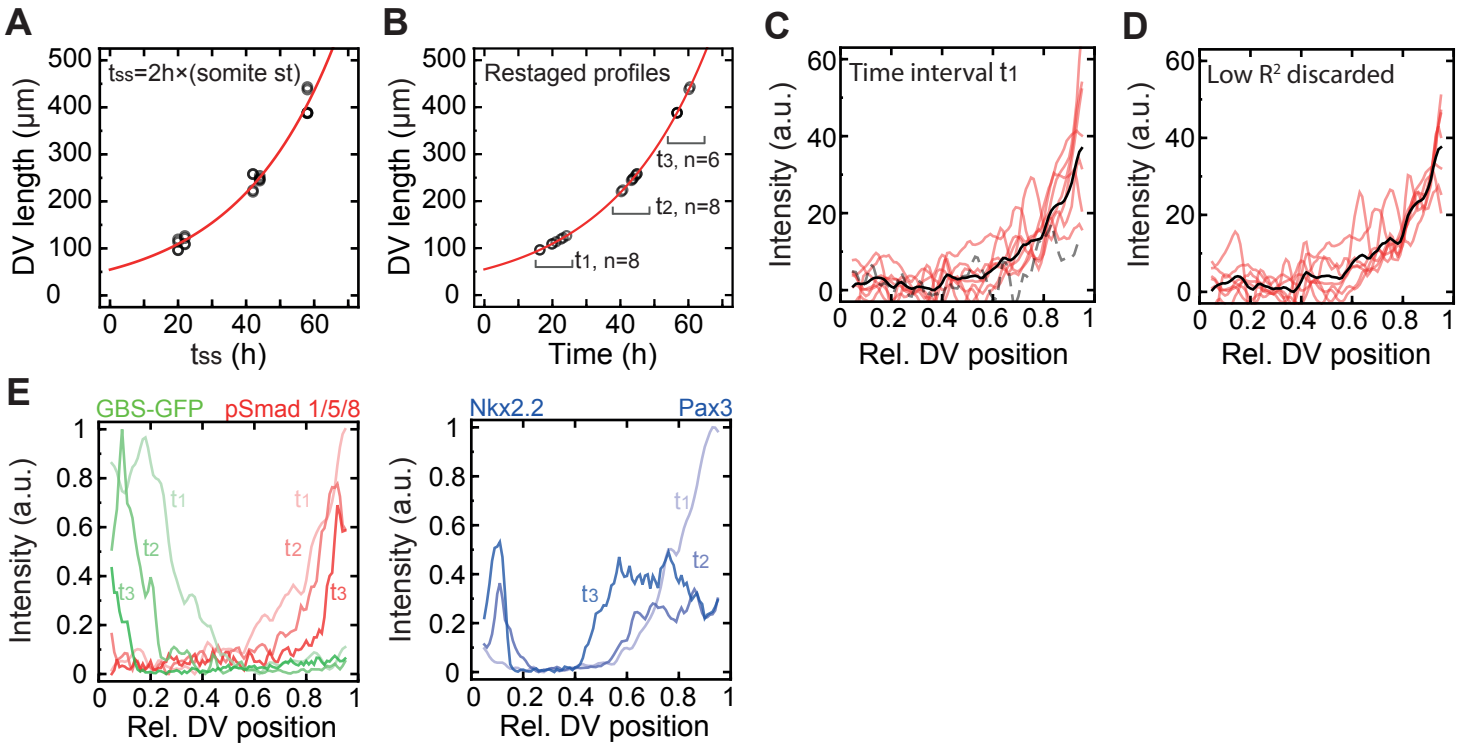
A
tss=2h×(somite st)
DV length (μm)
tss (h)
B
Restaged profiles
t3, n=6
t2, n=8
t1, n=8
DV length (μm)
Time (h)
C
Time interval t1
Intensity (a.u.)
Rel. DV position
D
Low R² discarded
Intensity (a.u.)
Rel. DV position
E
GBS-GFP
pSmad 1/5/8
t1
t2
t3
Intensity (a.u.)
Rel. DV position
Nkx2.2
Pax3
t1
t2
t3
Intensity (a.u.)
Rel. DV position